## VIBRATORY DRIVING OF A MONOPILE AT A NORTH SEA SITE

Holeyman A. UCLouvain, Belgium, 011-32-479 29 34 71, alain.holeyman@uclouvain.be Whenham V., Besix (formerly Fugro Geoconsulting), Brussels, Belgium, vwhenham@besix.com
Peralta P., Fugro USA Marine, Norfolk, United States, p.peralta@fugro.com
Ballard, J.-C., Fugro Geoconsulting, Brussels, Belgium, jc.ballard@fugro.com
Chenicheri Pulukul S., Shell U.K. Limited, Aberdeen, United Kingdom,

#### **ABSTRACT**

s.chenicheripulukul@shell.com

This paper presents the outcomes of a post-installation study performed for the vibrohammer installation of a monopile at a platform located in the Dutch Sector of the North Sea. The monopile diameter was 4.7 m with a length of 40.5 m. The target penetration depth was 31.5 m below seafloor (BSF). The subsoil consisted of very dense fine to medium sands locally with few thin strata of silty sand and sandy silt. During the installation of the monopile, early pile refusal was encountered. The pile installation was subsequently completed using an impact hammer. This paper aims to highlight the importance of monitoring during pile installation and to review key parameters affecting the vibratory driving installation process.

Keywords: monitoring, vibratory driving, hammer installation, monopile

#### INTRODUCTION

A conductor monopile foundation with diameter 4.7 m and length 40.5 m was to be installed through vibratory driving at a platform site located in the Dutch Sector of the North Sea. The target penetration depth was 31.5 m below seafloor (BSF). Before pile installation, the feasibility of installing the monopile to target depth using the specified vibrohammer (type CV-960-12 with nominal frequency 23.3 Hz) was assessed applying the Hypervib-1 method (Holeyman et al., 1996). The prediction highlighted the risk of early pile refusal in case of effective hammer frequency reduction due to insufficient power of the power pack (Holeyman et al., 2020). During the installation of the monopile, early pile refusal was encountered with the mobilized vibrohammer achieving only 25 m pile penetration due to hydraulic power pack failure. The actual maximum mobilized frequency of the CV-960-12 vibrohammer was recorded as lower than nominal. On this basis, a post-installation study was performed with the aim to improve on vibratory installation analysis methods, to gain confidence in future vibratory predictions, and to reduce operational costs for future installation projects.

#### **SOIL CONDITIONS**

The site is characterized by Holocene and younger Pleistocene sands covering an Elster infilled glacial valley. The Holocene deposits form the top marine sands with thickness around 2 m BSF, underlain by dense to very dense, silty sand layers. The soil conditions and stratigraphy were mainly based on one CPT correlated with information from a borehole located 7 m from the CPT and 8 m from the center of the monopile. Table 1 presents a summary of the interpreted soil conditions and stratigraphy at the platform location, indicating predominantly medium dense to very dense sand layers with a 2 m thick silt layer below the marine sands. The cone tip resistance profile  $q_c$  and friction ratio profile  $R_f$  from the CPT are provided on Figure 1.

Table 1. Summary of Soil Conditions at the Platform Site

Depth Range of Soil Units (BSF) [m]	General Soil Conditions	Likely Geological Formation
0.0 to 2.5	Medium dense to very dense, locally silty, fine to medium SAND	Holocene marine sand (Twente Formation)
2.5 to 4.5	Medium to high strength, clayey SILT	Eem Formation
4.5 to 33	Dense to very dense SAND	Eem Formation
33 to > 40	Medium dense to dense, silty SAND	Eem, Tea Kettle Formations

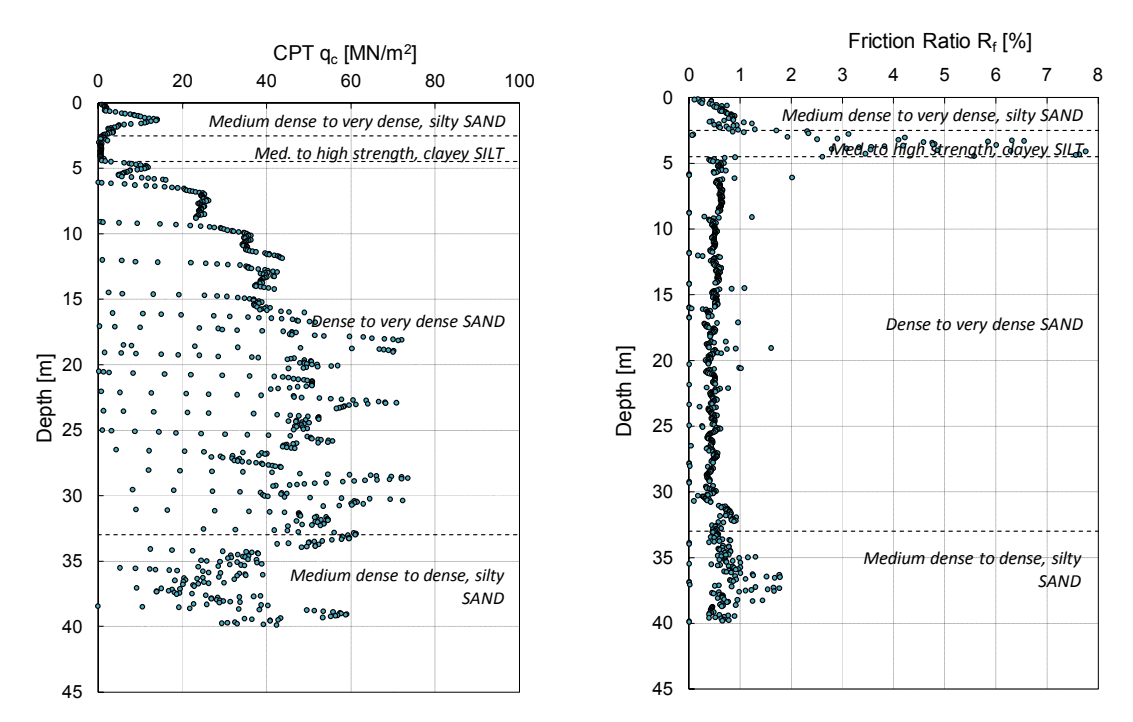


Fig. 1. CPT cone tip resistance and friction ratio at the site

## HAMMER CHARACTERISTICS AND INSTRUMENTATION

A customized CV-960-12 VLT vibrohammer was used for the vibratory driving. Table 2 summarizes the vibrohammer specifications. Pile driving monitoring (PDM) during installation of the monopile was performed and included accelerometers and strain gauges set at a distance of one diameter from the pile head. Table 3 summarizes the measured parameters during vibratory driving, together with the associated instrumentation and sampling rates. The monopile outer diameter was 4.7 m with a total length of 40.5 m. The wall thickness (WT) varied from 50 mm at the toe to 85 mm at the head with the pile divided into 4 sections. Its nominal dry weight was 354 tons.

**Table 2. Vibrohammer Specifications** 

Property	Value
Type Number of vibrators Number of clamps Frequency, f [Hz] Angular frequency, ω [rad/s] Total eccentric moment, me [kg.m] Total centrifugal force, F <sub>c</sub> [kN]	CV-960-12 VLT 3 8 23.3 146.4 960 20 575
Total dynamic mass [kg] Static mass upending [kg]	161 000 71 000
crane mace aponania [ng]	

Table 3. Measured Parameters during Vibratory Driving and Associated Instrumentation

Parameter	Instrumentation	Sampling rate
Frequency	Two piezoresistive accelerometers and two strain gauges	3125 Hz
Accelerations	Two piezoresistive accelerometers	3125 Hz
Strains (forces)	Two strain gauges	3125 Hz
Oil flow and oil pressures (in & out) from the hydraulic power pack /pump system	Pressure sensors located on the hydraulic power units and on the manifold box Oil flow rate sensor located on the hydraulic power units	1 Hz

## VIBRATORY DRIVING INSTALLATION

## **Depth Measurements**

Figure 2 presents depth measurements during vibratory driving. Self-weight penetration was observed up to 4 m BSF through the top sand and silt layers. High penetration velocities were observed between 4 m and 10 m BSF. A first drop in penetration velocity was observed around 11 m BSF. That first decrease was counteracted by an adjustment of the vibrator power pack operating parameters. Power was incremented a second time towards 15.7 m BSF to accelerate penetration, but a second drop in penetration speed was observed at 22.5 m BSF. Refusal was reached at a depth of 25.0 m.

## Accelerometers and Strain Gauges Measurements

The acceleration and force measurements, deduced from the PDM signals, can be decomposed into static and vibratory components. The static component corresponds to the mean value of the signals over a given time period. The vibratory (dynamic) component corresponds to the alternating part of the signals. Figure 3 presents examples of accelerometer and strain gauge transducers signals for penetration depths of 9.75 m and 24.5 m BSF, after removal of the static component (zero frequency of the signals).

Accelerometers and strain gauge transducers show a frequency content diagram highly dominated by the driving frequency applied by the vibrator. Figure 4 presents the dominant

driving frequencies deduced from the acceleration measurements, along with interpreted frequencies provided by the contractor.

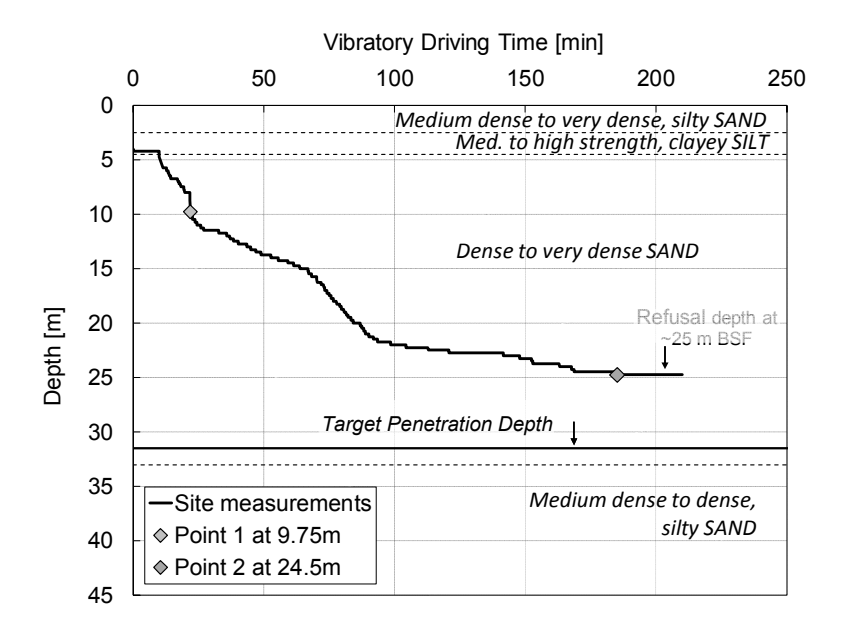


Fig. 2. Depth measurements during vibratory driving

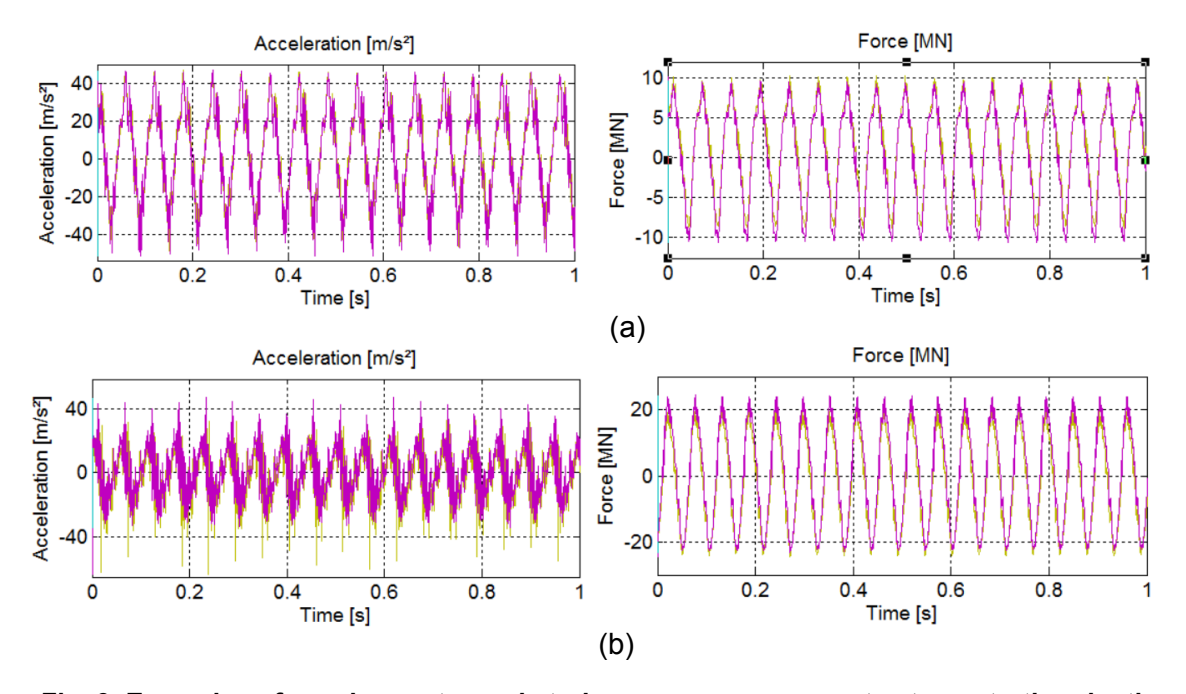


Fig. 3. Examples of accelerometer and strain gauge measurements at penetration depths of (a) z = 9.75 m BSF and (b) z = 24.5 m BSF

The dominant frequency ranged between 16 Hz and 19 Hz, i.e. significantly lower than the nominal value of 23.3 Hz (see Table 2). On top of the dominant frequency, harmonic frequencies are present both in acceleration and force signals. Higher frequencies are generally more developed when approaching refusal, indicating that the vibrations struggle to achieve a steady state condition.

The acceleration and vibratory force amplitudes have been derived assuming that the acceleration and strain gauge signals are mostly harmonic and after filtering out frequencies above 30 Hz and 350 Hz, respectively.

From the acceleration amplitudes, displacement amplitudes (i.e. vibratory component of the movement) can be calculated by double integration, assuming that the mean acceleration is nil on average and that velocity is constant within a period. The resulting harmonic displacement amplitude is presented on Figure 4(b) as a function of the penetration depth. These results can be compared with the nominal amplitude of vibration usually taken as

$$d_0 = me/M_{dyn} ag{1}$$

where  $M_{dyn}$  is the dynamic mass (vibrating part of the vibrator, clamp and pile) [kg] and me is the eccentric moment of the vibrator [kg.m]. The above equation implicitly assumes that the monopile behaves as a rigid body.

Figure 4(b) also presents the expected range of displacement amplitudes at a distance of 4.7 m from the pile head for an elastic pile as bracketed by two extreme boundary conditions (free and fixed pile toe conditions respectively corresponding to "very low" and "very high" soil resistance concentrated at the pile toe). The analytical solution (Whenham and Holeyman, 2012) corresponding to the "fixed base" condition helps understanding the significant decrease in displacement amplitude observed below 22.5 m BSF. Attention should be paid to the fact that the displacement amplitudes presented herein are based on measurements performed at a distance of 4.7 m from the pile head. Under refusal conditions, it can be expected that the decrease in displacement amplitude is even more significant close to the pile toe.

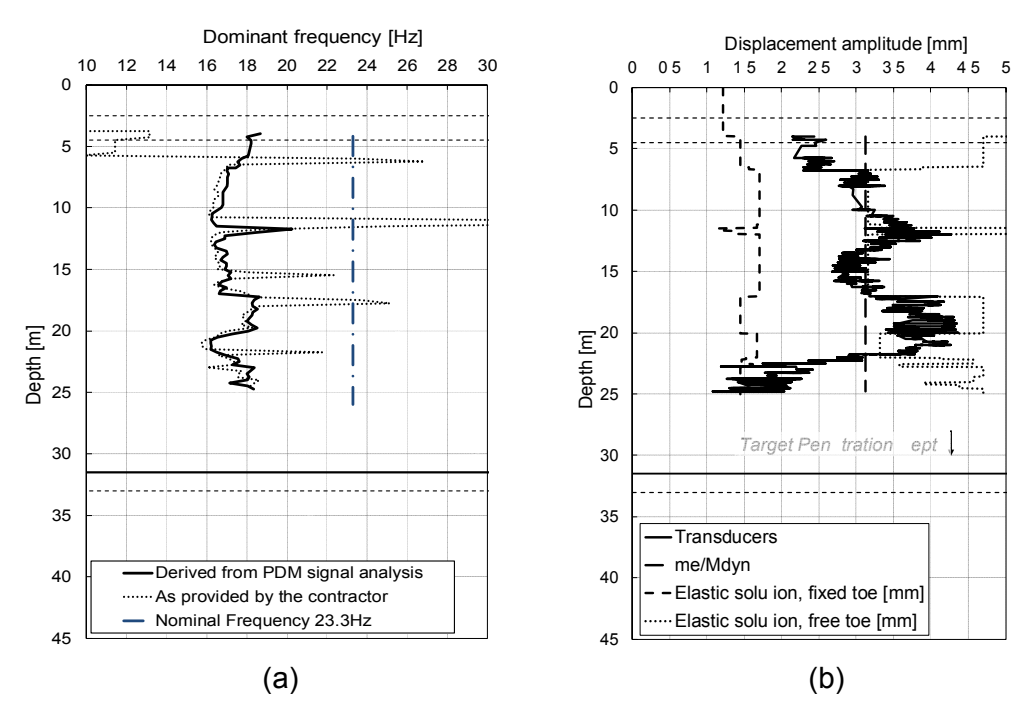


Fig. 4. Dominant frequency (a) and harmonic displacement amplitude (b) at monopile head ( $z_p = 4.7m$ ) as functions of penetration depth

On Figure 5, the amplitude of the alternating part of the force signals (vibratory force) is compared with the pile centrifugal force determined from the specified moment eccentricity me multiplied by the square of the current angular frequency. The difference between the pile nominal centrifugal force and the amplitude of the vibratory force measured by the strain

gauge transducers can be explained by the mechanical interaction between the vibrator and the sometimes called "effective" mass of the elastic pile (Whenham and Holeyman, 2012).

The expected range of axial forces transferred to the monopile at 4.7 m from the pile head is also bracketed on Figure 5 assuming two extreme boundary conditions, i.e. a free and a fixed pile toe condition corresponding to "very low" and "very high" soil resistance concentrated at the pile toe, respectively. The force transferred onto the pile as derived from strain gauge measurements generally increases with the penetration depth, reflecting the general increase in soil resistance. The analytical solution based on the 'free base' assumption fits with field measurements upon starting at 4 m BSF, whereas the analytical solution considering the "fixed base" assumption corresponds well to field measurements as refusal is approached.

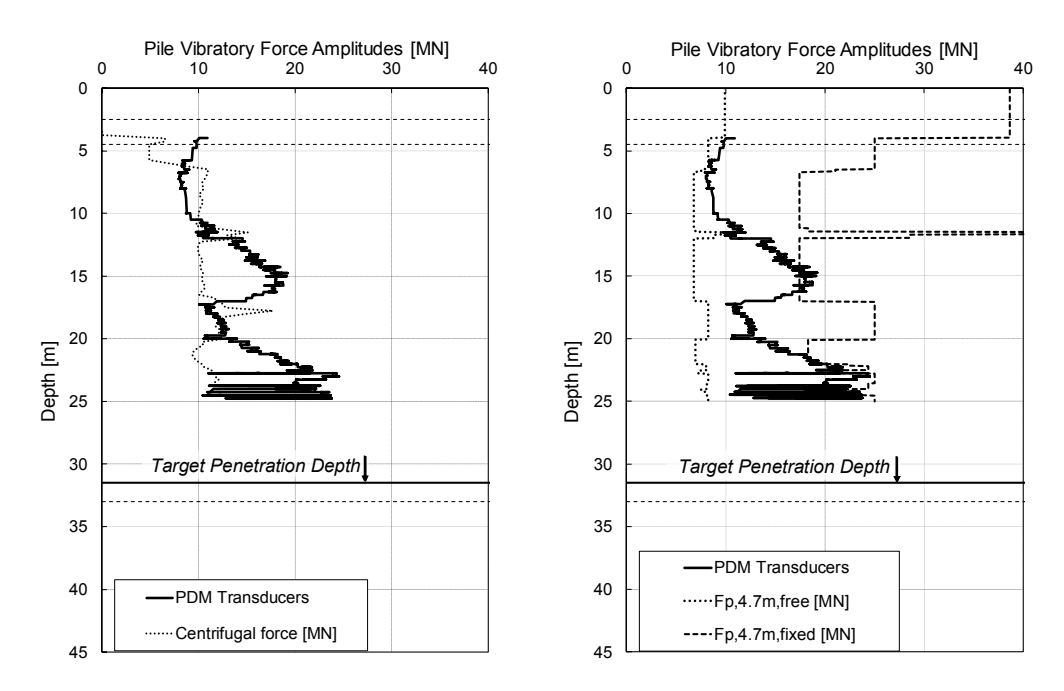


Fig. 5. Vibratory force amplitude as a function of penetration depth

## Oil Flow and Oil Pressure Measurements

The hydraulic power developed by the hydraulic power pack can be compared to the mechanical power transmitted to the monopile, as shown on Figure 6. On Figure 6, the power developed by the hydraulic pack is deduced from the oil flow rate and oil pressure measurements using:

$$P_{hvdr} = (p_{out} - p_{in}). Q. \cos \varphi$$
 [2]

where  $p_{out}$  and  $p_{in}$  are the oil pressures leaving and entering the hydraulic power pack, respectively, Q is the oil flow rate, and  $\cos \varphi$  is the efficiency factor of the hydraulic motor (assumed to be equal to unity). The mechanical power transmitted to the pile head is estimated based on the PDM signals using a time-averaged form of the fundamental relationship:

$$P_{mech} = Force(t).Velocity(t)$$
 [3]

where Force(t) and Velocity(t) are the total (static + harmonic) forces and velocity measured at the monopile head ( $z_p = 4.7 \text{ m}$ ).

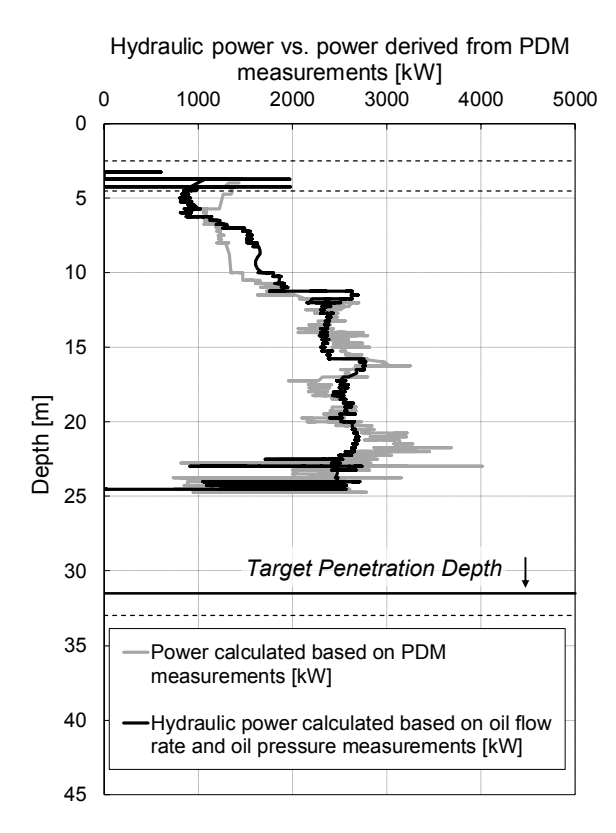


Fig. 6. Comparison between hydraulic power developed by the powerpack and mechanical power transmitted to the monopile, as deduced from PDM measurements function of penetration depth

# BACK-ANALYSIS OF VIBRATORY SOIL RESISTANCE AND COMPARISON WITH INITIAL PREDICTIONS

The installation predictions consisted in an assessment of vibratory soil resistance (VSR) and an estimation of the penetration rate and dynamic stresses during driving. The penetration depth of the monopile was estimated by comparing the effective force transmitted to the pile to the soil resistance under vibratory action (or VSR). The Hypervib-1 method developed by Holeyman et al. (1993, 1994, 1996) was applied to estimate the soil resistance to vibratory action and penetration velocities. Details of the design basis and methodology are provided in Holeyman et al. (2020).

## Back-Analysis of Vibratory Force Transfer

In the initial predictions, the force amplitude transmitted to the pile  $F_p$  was assessed from 1D wave equation analysis using the software program GRLWeap (PDI, 2010). The calculations were performed at discrete penetration depths covered by the expected driving process. The results appeared to be very sensitive to small changes in soil and/or vibratory hammer parameters. In view of the uncertainties inherent to the GRLWeap model, the force amplitude adopted in the initial Hypervib predictions was chosen as the average value of the force amplitude modelled close to the pile toe (actually the maximum force amplitude along the pile) obtained from the depth of self-weight penetration (about 5 m) to the target depth of 31.5 m.

Table 4 presents the calculated  $F_{p,x=4.7m}$  values adjusted to cover the range of frequencies actually monitored at the position of the strain gauge transducers (x = 4.7 m from pile head).

The calculated force amplitudes are compared to the nominal pile centrifugal force  $F_c$  of the CV-960 VLT vibrohammer and to the force amplitudes transmitted to the pile at x = 4.7 m as derived from the strain gauge measurements. Figure 7 illustrates the calculated vibratory force amplification profile along the pile (ratio between the vibratory force calculated at a distance x from the pile head and the vibratory forces calculated at the pile head) for a pile penetration depth of 24.5 m, under an operating frequency of 17 Hz.

Table 4 highlights the uncertainties associated with the assessment of the force amplitude transmitted to the pile during vibratory driving. The forces amplitudes developed along the pile can vary with a factor 2 or 3 depending on the soil resistance, driving frequency and distance to the pile head. In the range of 16 to 19 Hz, the 1D wave equation analysis shows limited influence of the driving frequency on the vibratory force amplitudes transferred to the pile. This observation is validated by the field data that show that the forces measured by the strain gauge transducers are more influenced by the soil resistance than by the driving frequency (Figures 4 and 5). The calculations performed using GRLWeap software also indicate that the axial forces amplitudes are highly dependent on the distance to the pile head, as illustrated on Figure 7 for a driving frequency f = 17 Hz.

Table 4. Vibrohammer Frequency and Pile Centrifugal Force

Hammer Frequency f [Hz]	Nominal Pile Centrifugal Force F <sub>c</sub> , [MN]	Calculated Force at 4.7m from Pile Head[MN] <sup>(1)</sup>	Measured Force at 4.7m from Pile Head [MN] <sup>(1)</sup>
19	14	9 to 16	10 to 22
18	12	8 to 17	8 to 24
17	11	7 to 17	7 to 21
16	10	8 to 17	7 to 22

<sup>(1)</sup> Minimum and maximum values from the depth of self-weight penetration to the refusal depth (25.5 m)

## Back-Analysis of Vibratory Soil Resistance

The VSR considered for the initial prediction was calculated assuming coring behavior and using the soil profile and friction ratio from the CPT (Figure 1).

The soil degradation parameters considered for defining both best estimate (BE) and high estimate (HE) of the VSR corresponded to the recommendations made by Holeyman & Whenham (2017). The BE and HE VSR adjusted for the hammer frequency and vibratory forces actually applied to the pile are presented on Figure 8, together with the theoretical and measured pile forces acting on the pile (at a distance of 4.7 m from pile head).

The theoretical "static" force  $F_s$  corresponds to sum of the weight of the upper segment of the monopile and of the total weight of vibratory hammer, including clamps and hydraulic hoses. The theoretical "centrifugal" force  $F_c$  is determined from the specified eccentric moment me (Table 2) multiplied by the square of the angular frequency  $\omega$ , corrected for a representative driving frequency f = 17.5 Hz.

The "measured" pile force  $F_{mes,toe}$  is derived from the amplitude of the alternating part of the force signals (vibratory force) measured by the strain gauge transducers and corrected by the pile vibratory force amplification factor at the pile toe (Figure 7). Using BE parameters, the sum of the theoretical centrifugal and theoretical static forces applied to the pile ( $F_c + F_s$ ) crosses the VSR profile at 17 m BSF, indicating earlier refusal depth than actually observed.

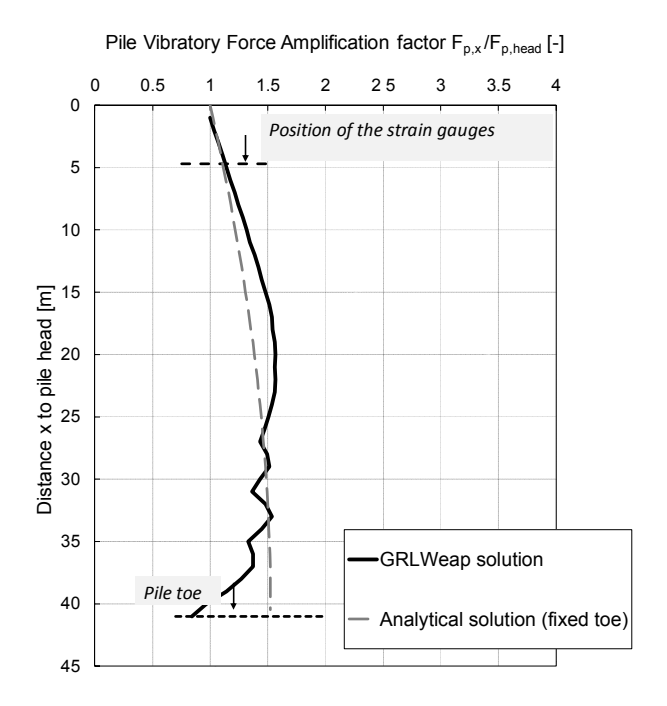


Fig. 7. Force amplification factor along the pile as calculated using GRLWeap software program for a driving frequency f = 17 Hz, at penetration depth = 24.5 m

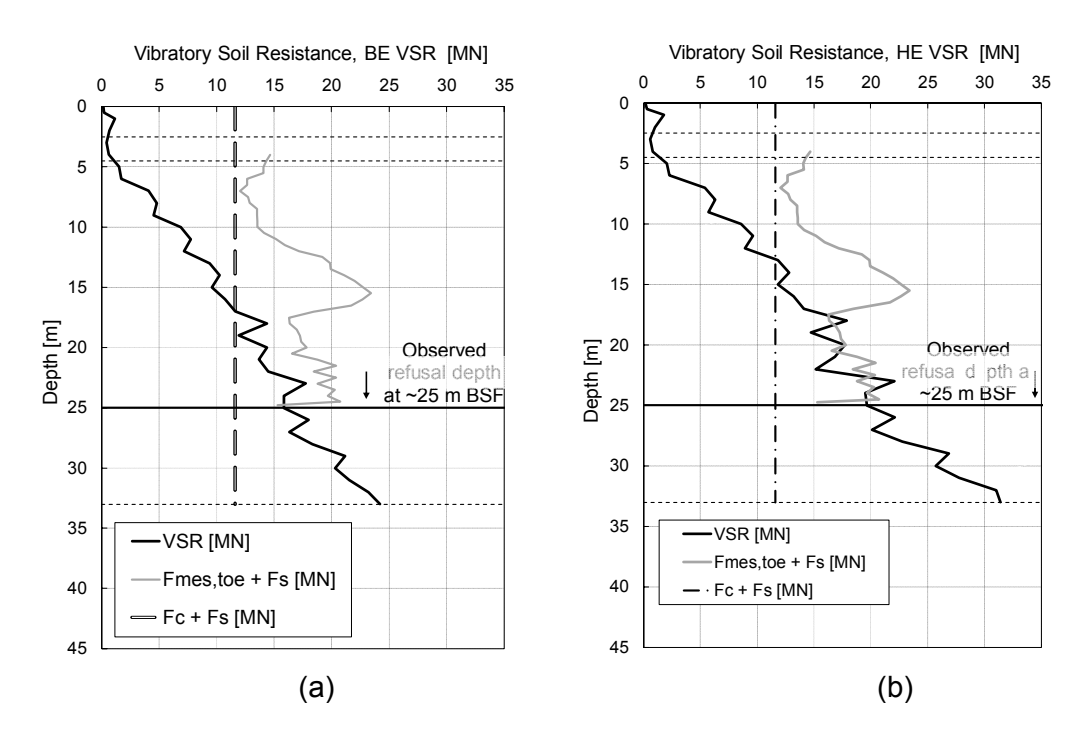


Fig. 8. BE VSR (a) and HE VSR (b) curves adjusted on frequency and vibratory force measurements

On the other hand the refusal depth is correctly predicted when using BE parameters and adjusting the vibratory force amplitude based on strain gauge transducer measurements corrected by the pile vibratory force amplification factor at pile toe ( $F_{mes,toe} + F_s$  curve). Using the HE parameters, the sum of the theoretical centrifugal and static driving forces applied to the pile ( $F_c + F_s$ ) crosses the VSR profile at 13 m BSF, while the measured sum of cyclic and static driving forces ( $F_{mes,toe} + F_s$ ) crosses the VSR profile at 17 m BSF.

## **SUMMARY AND CONCLUSIONS**

This paper reviews the instrumentation monitoring data acquired during the vibratory installation of a 4.7 m diameter monopile foundation. On this basis, driving parameters and performance were re-assessed and compared with initial predictions. Main conclusions are as follows:

- 1) The early refusal encountered during vibratory installation is likely mainly due to the fact that the driving frequency was significantly lower than that considered for the drivability predictions (Holeyman et al. 2020). Other factors not covered by current model capabilities may have contributed to the early refusal such as the damping effect of the soil on the elastic response of the monopile, the vibratory force actually transferred onto the pile, and the hook force exerted by the crane operator during vibratory driving.
- 2) The driving force actually transmitted to the pile is a key factor affecting vibro-drivability. While analytical solutions (Whenham & Holeyman 2012) and 1D wave equation (PDI, 2010) help define upper and lower bounds of the driving force, the models currently available do not allow for an accurate assessment of the driving force. The uncertainties in estimating the driving force amplitudes should therefore be considered in vibratory drivability assessments.
- 3) The Hipervib1-method gives satisfactory although slightly conservative predictions of refusal depth. The main uncertainties affect the assessment of the vibratory driving force actually applied to the pile and the magnification of the vibratory forces along the pile.

#### **ACKNOWLEDGMENTS**

The first author acknowledges the support of Fugro Geoconsulting Belgium to prepare this paper. The post installation study was performed by Fugro Geoconsulting Belgium for Shell UK. The contractor in charge of the installation of the monopile was Cape Holland. The instrumentation specialist was Allnamics in the Netherlands.

## **REFERENCES**

Holeyman, A. (1993). HIPERVIB1, An analytical model-based computer program to evaluate the penetration speed of vibratory driven sheet piles, Research report prepared for BBRI, 25p.

Holeyman, A. Legrand, C. & Van Rompaey, D. (1994). Soil Modeling for Pile Vibratory Driving. International Conference on Design and Construction of Deep Foundation; Orlando, Florida, Vol.2, pp.1165-1178.

Holeyman, A. Legrand, C. & Van Rompaey, D. (1996). A Method to Predict the Drivability of Vibratory Driven Piles. Stress Wave '96, September 1996, Orlando: Townsend, F.C, Hussein M., and Mc Vy M.C., pp.1101-1112.

Holeyman, A., Whenham, V. (2017). Critical review of the Hypervib1 model to assess pile vibro-drivability. . Geotech.Geol.Eng.3, 1-19.

Holeyman, A., Whenham, V., Peralta, P., Ballard, J.-C., Chenicheri Pulukul, S. (2020). Vibratory Installation Study of a Monopile in dense Sand, Proceedings of the OMAE 2020 Conference, June 28 – July 3, Fort Lauderdale, FL, Paper # 19204.

PDI (2010). GRLWEAP User's Manual. Cleveland: Pile Dynamics, Inc.

Whenham, V. & Holeyman, A. (2012). Load Transfer during Vibratory Driving. Geotechnical and Geological Engineering, October 2012, Volume 30, Issue 5, pp.1119-1135.